Original article

Morphological characteristics of the rat thymus during perinatal protein deprivation and early refeeding: a qualitative and quantitative study

Baptista, JS.[1]*, Mayer, WP.[1], Fontes, R.[2], Seyfert, CE.[3], Boldrini, SC.[4] and Liberti, EA.[5]

[1]Assistant Professor, Human Anatomy Division, Department of Morphology, Federal University of Espirito Santo – UFES, Maruipe Avenue, 1468, 29043-900, Vitoria, ES, Brazil
[2]Rush University Medical Center, 1725 West Harrison, Suite 1115, Chicago, IL, 60612, USA
[3]Life Sciences Academic Unit, Federal University of Campina Grande – UFCG, Sérgio Moreira de Figueiredo Street, 58900-000, Cajazeiras, PB, Brazil
[4]Associate Professor, Department of Anatomy, University of Sao Paulo – USP, Prof. Lineu Prestes Avenue, 2415, 05508-900, Sao Paulo, SP, Brazil
[5]Full Professor, Department of Anatomy, University of Sao Paulo – USP, Prof. Lineu Prestes Avenue, 2415, 05508-900, Sao Paulo, SP, Brazil
*E-mail: josemberg.baptista@ufes.br

Abstract

Protein malnutrition is particularly deleterious in young individuals. An immunodeficient state is a well-known functional consequence but alterations in thymic morphology remain unknown. Our aim is to analyze morphological characteristics of the rat thymus in a perinatal undernutrition and renutrition model – we hypothesize these morphological alterations are reversible with early refeeding. Ninety-day-old Wistar rats were allowed to mate and divided into three groups: nourished (N – normal 20% protein diet), undernourished (UN – pre- and postnatal 5% protein diet until post-natal day 60 – PND 60) and renourished (RN – as UN but normal diet from PND 21 to 60). The thymi of 10 pups/group were submitted to macroscopic, histology, morphometry and scanning electron microscopy analyses. Body weight was highest in N and lowest in UN animals as expected but the thymic/body weight ratio remained similar in N and UN; this ratio was significantly higher in the RN group. UN thymi had a prevalence of type I collagen fibers, atrophic lobules and absence of a clear corticomedullary boundary. Thymic cortical component was decreased in UN. Apoptotic thymocytes were more frequently visualized in the UN thymi. N and RN thymi exhibited very similar morphology. Perinatal protein malnutrition induces drastic morphological alterations in rat thymi but these could be largely reversed with early renutrition. Functional studies are needed to assess if organ function mimics morphology in its recovery.

Keywords: malnutrition, proteins, thymus, anatomy and histology, rats, Wistar.

1 Introduction

ialnourishment is a multifactorial condition with elevated prevalence in developing countries - it is unnecessary to further point out its importance and burden to their populations (SLOBODIANIK, PALLARO, ROUX et al., 1989). The perverse consequences of early protein malnourishment have been known to man for centuries: several nutritional instructions are found in ancient texts and the term "*kwashiorkor*" lends itself as living witness to this historical fact. Lymphoid consequences of nutritional deficiencies were first reported in the literature in the early 19th century: Johann Friedrich Meckel the Younger described thymic atrophy secondary to malnourishment in 1810. John Simon further explored thymic atrophy in his seminal 1845 essay on the thymus – the term "nutritional thymectomy" was incorporated into medical use thereafter (BEISEL, 1992; SIMON, 1845).

The interest in nutritional immunology steadily grew in the last 40 years not only because of alarming numbers of impoverished, malnourished individuals in developing countries but also because of the increasing number of patients in high-complexity medical centers of developed countries suffering from secondary immunodeficiency related to nutrition such as in trauma or cancer cachexia. Several components of both cellular and humoral-mediated immunity are known to be affected in protein malnourishment: circulating lymphokines, complement proteins, T lymphocyte and neutrophil numbers are all decreased while immunoglobulin levels are normal or slightly elevated. Furthermore, other functional components of the immunological response such as neutrophil function, phagocytosis and the whole inflammatory process itself are impaired. Malnourishment does not lead only to a decreased immunological response: other problems of dysfunctional response such as allergies and autoimmune disorders may also be induced (BEISEL, 1992; CHANDRA and CHANDRA, 1986; REVILLARD and COZON, 1990; SLOBODIANIK, PALLARO, ROUX et al., 1989). Immunological comprise is particularly deleterious in the pediatric age range: a survey by

Schofield and Ashworth (1996) in 67 different countries found 20-30% median mortality rates among children hospitalized due to severe protein-energy malnutrition. Most of these deaths (56%) are caused by secondary infections, particularly of the respiratory and digestive tracts (PELLETIER, 1994; SCHOFIELD and ASHWORTH, 1996).

Even though thymic atrophy was described in the early 19th century, research into the morphology of this organ during malnourishment was lacking until pioneering reports were published in the 1970s. Mugerwa (1971) further detailed thymic atrophy in children with kwashiorkor and reported for the first time on the loss of the corticomedullary boundary and decrease of thymic corpuscles. He was followed by the reports of Weindruch and Suffin (1980) and Mittal and Woodward (1985), which examined additional thymic characteristics in classic malnutrition and revealed now-classic features such as increase of the thymic/corporal weight ratio, intracytoplasmic accumulation of cholesterol and thymocyte depletion. A comprehensive analysis of thymic morphology, however, was precluded by the heterogeneity of their malnourishment models: every one of these reports utilized models with different protein-energy characteristics (MITTAL and WOODWARD, 1985; MUGERWA, 1971; WEINDRUCH and SUFFIN, 1980). A subset analysis of protein-restriction models yields only a limited number of publications. Mittal, Woodward and Chandra (1988) reported a thymic cortex:medulla ratio of 2:1 and thymocyte depletion in protein-restricted rats – these results were also common to protein-energy-restricted animals. Barone, O'Brien and Stevenson (1993) demonstrated elevated serum corticosteroid levels during malnutrition and correlated them to thymic atrophy and thymocyte depletion. Savino and Dardenne (2010) have recently reviewed thymic alterations in several malnourishment states; specifically, the atrophy secondary to protein-energy malnourishment results in thymic atrophy through a depletion of immature CD4+/CD8+ cells. In spite of these recent studies, to the authors' knowledge no studies have been performed on a pre- and post-natal model of protein malnourishment. This model would be particularly useful in light of the controversy whether the above-mentioned thymic alterations may become permanent/chronic and persist into adulthood (DOUROV, 1986) or are reversible with restoration of normal nutrition (BARONE, O'BRIEN and STEVENSON, 1993). While this discussion lingers predominantly on physiological aspects, studies concerning the morphological alterations associated with mal- and renourishment are still lacking.

The objective of this study is therefore to examine morphological characteristics of the rat thymus in a pre- and post-natal protein malnourishment model and to answer whether these modifications are reversible upon normal renourishment. Additional analyses are also performed on thymic and corporal weight dynamics under mal-/renourishment conditions.

2 Material and methods

This experimental study was developed at the Department of Anatomy, Instituto de Ciencias Biomedicas da Universidade de Sao Paulo, Brazil, from January 2007 to December 2010. All experiments were approved by the Ethics Commission on Animal Experiments of the Instituto de Ciencias Biomedicas da Universidade de Sao Paulo (No. 031/2007). After initial approval, yearly and final reports were required and also approved; these analyses ensured that compliance with the Brazilian legislation on animal experiments was observed during the entire study period.

A widely-used perinatal model of parent and pup protein undernutrition was employed (GREGGIO, FONTES, MAIFRINO et al., 2010; LIBERTI, FONTES, FUGGI et al., 2007; REEVES, NIELSEN and FAHEY, 1993). Young adult (90-day old) male and female Wistar rats were allotted to nourished and undernourished groups (WALKER, NAKAMURA and HODGSON, 2010). The nourished group received their usual AIN-93G diet with 20% casein (Rhoster, Sao Paulo, Brazil) while the undernourished group was fed a modified low-protein AIN-93G (5% casein – Rhoster). They were kept under these conditions for 7 days and allowed to mate. Standard conditions were maintained throughout the experiment at 23-25 degrees Celsius, 12-hour light/dark cycle with water and food *ad libitum*.

After conception was confirmed, the females were placed in individual cages while still being fed their predetermined diet. The nourished group received the **N** denominator while the animals receiving the low-protein diet were randomly divided into undernourished (**UN**) and renourished (**RN**) groups. The pre-assigned diet was still fed to the dams and pups until the end of the weaning period (post-natal day 21 – PND 21). At the end of this period, the pups of all groups were separated from the dams and the **RN** group had its diet switched to the regular protein AIN-93G. Ten pups from each group were randomly selected when they reached the pubescent stage (PND 60) and euthanized with an overdose of sodium pentobarbital. Corporal and thymic weights were obtained.

2.1 Macroscopic and low-power magnification analyses

Two specimens from each group were randomly selected and submitted to fixation with 4% formaldehyde for 72 hours. They were then immersed in toluidine blue for 10 minutes and washed in phosphate-buffered saline (PBS). These specimens were examined macroscopically and under low-power magnification (3-5×) (Stemi SV6 loupes, Carl Zeiss GmbH, Jena, Germany).

2.2 Light microscopy analysis

Five specimens from each group were selected and fixed with 4% formaldehyde for 72 hours. Dehydration through a series of increasing-grade ethanol (80-90-100%) and xylene was performed. Semi-serial (one in ten) 6 µm-thick paraffin-embedded sections were then obtained through the area of largest diameter of the thymus. Routine histology staining followed and slides were analyzed under different magnifications (Axioscope 40, Carl Zeiss GmbH, Jena, Germany). Histology techniques employed were hematoxylin and eosin (HE) for a general histological analysis and Sirius-Red for collagen fiber examination (ROMEIS, 1968). Sirius-Red staining and subsequent analysis of collagen birefringence allows easy differentiation between the three fibrillary collagens in large tissue samples based on their individual fiber length: types I (strong yellow and red birefringence), II (weak birefringence, barely standing out

from amorphous ground substance) and III (intermediate greenish birefringence) are thus detectable under polarized light (JUNQUEIRA, TOLEDO and MONTES, 1981; MELROSE, SMITH, APPLEYARD et al., 2007; MONTES, KRISZTÁN and JUNQUEIRA, 1985; SWEAT, PUCHTLER and WOO, 1964).

2.3 Scanning Electron Microscopy (SEM)

Three thymi from each group were selected and fixed in Karnovsky's medium (SCHNEEBERGER-KEELEY and KARNOVSKY, 1968) for 48 hours at 4 degrees Celsius. These thymi were then washed in PBS and cryofracture was achieved through immersion in liquid nitrogen for 30 seconds. The specimens were then post-fixed in 1% osmium tetroxide, critical point-dried (Bal-Tec CPD-030, Liechtenstein), gold-coated (Balzers Union SCD-040 ion sputterer, Liechtenstein) and examined in a scanning electron microscope (Jeol JSM-6100, Tokyo, Japan) (MIYAI, ABRAHAM, LINTHICUM et al., 1976).

2.4 Quantitative analysis – Relative area and vessel density

The five thymi from each group selected for light microscopy analysis were also utilized for quantitative analyses. The following areas are identified in normal thymi: *thymic cortex* (TC), *thymic medulla* (TM) and *non-lymphoid tissue* (NLT – vessels, capsule and interlobular septae) (LIBERTI, VILLA, MELHEM et al., 1989). Thirty sections on a major cross-section area of each thymi were examined under low-power magnification and the areas of the total thymic section and its components measured with imaging-analysis software (Axiovision 4.6, Carl Zeiss Microimaging, Jena, Germany). The area fraction taken up by each component was assessed by point counting on a test system with equidistant 300 test points (P_T) superimposed on the total area of the photomicrographs (MANDARIM-DE-LACERDA, 1995). *Vessel density* (V_V) was assessed in the medulla because of the well-known mechanism of mature T-cell migration into the circulatory system (SAVINO and DARDENNE, 2000). Five random microscopy fields were acquired at 40× magnification in each thymic section and vessel density calculated utilizing the 150 trace counting after-test system as described above (WEIBEL, 1979), on the same image analysis software. This procedure was repeated in 5 different thymic sections, five animals per group thus resulting in 125 microscopy fields analyzed per experimental group. The stereological coefficient was calculated and considered acceptable if less than 10%. All quantitative results were tested through ANOVA with statistical significance set at the 0.05 level. When a significant difference was detected, groups were tested against each other with Tukey's test (ZAR, 1999).

3 Results

3.1 Subjective assessment

Pups of the **UN** and **RN** possessed characteristics that distinguished them from the control **N** pups and are very similar to the phenotype of human protein malnourishment. Their hair was uniformly thinner and scarcer than that from **N** pups though this condition gradually reversed in **RN** pups as they were fed the normal diet. Pasty feces were also uniformly observed when **RN** animals underwent the first few days of renourishment. Besides being considerably smaller than **N** pups as shown in Table 1, **UN** animals had virtually no subcutaneous fat and their musculature was considerably hypotrophic at day 60. Their abdominal wall in particular was so hypotrophic that intraabdominal organs were visible to the naked eye in striking contrast to the nourished animals. The sternum and ribs were also fragile and brittle; the tiniest effort was enough to open the thoracic cavity during dissection.

3.2 Corporal and thymic weights

Body and thymic weights for each of the three groups is shown in Table 1. Body weight was significantly decreased in the **UN** group but a significant degree of recovery was evident in the **RN** animals. **RN** animals did not, however, reach weights comparable to **N** controls. Thymus size is also represented as a percentage of total body weight in Table 1. While corporal and thymic weight loss during undernutrition are relatively proportional, thymic compensatory hypertrophy is evident even before corporal weight is back to normal – the difference between **N** and **RN** thymic weight, as opposed to corporal weight, was not statistically significant (Table 1). The compensatory hypertrophy of thymus is further evidenced by the differing thymic/corporal weight ratio in **RN** animals.

3.3 Macroscopic and low-power magnification (mesoscopic) analysis

Even though the thymi of the several groups were markedly different in size, the bilobar configuration was maintained across the three groups (Figure 1). The **UN** thymi were clearly distinct from the other 2 groups. One could not, however, differentiate **N** and **RN** thymi on macroscopic analysis only. Under low-power magnification, the thymic capsule of **N** animals exhibited a characteristic grooving pattern (Figure 2). The surface of **UN** thymi, however, was considerably flattened and the lobular grooves had disappeared. In contrast to their macroscopic appearance, **RN** thymi had a surface pattern that more closely resembled the **UN** thymi (Figure 2c). Even though lobular distinction had returned to some extent to its original state, its finer grooving pattern was still absent.

Table 1. Corporal and thymic weights at post-natal day 60, mean ± standard deviation.

	N	UN	RN
Body weight (g)	288.3 ± 15.8*	60.13 ± 15.0*	209.8 ± 16.2*
Thymic weight (g)	0.73 ± 0.16	0.15 ± 0.05*	0.83 ± 0.13
Thymic/body weight (%)	0.25 ± 0.05	0.26 ± 0.07	0.40 ± 0.06*

* – $p < 0.05$.

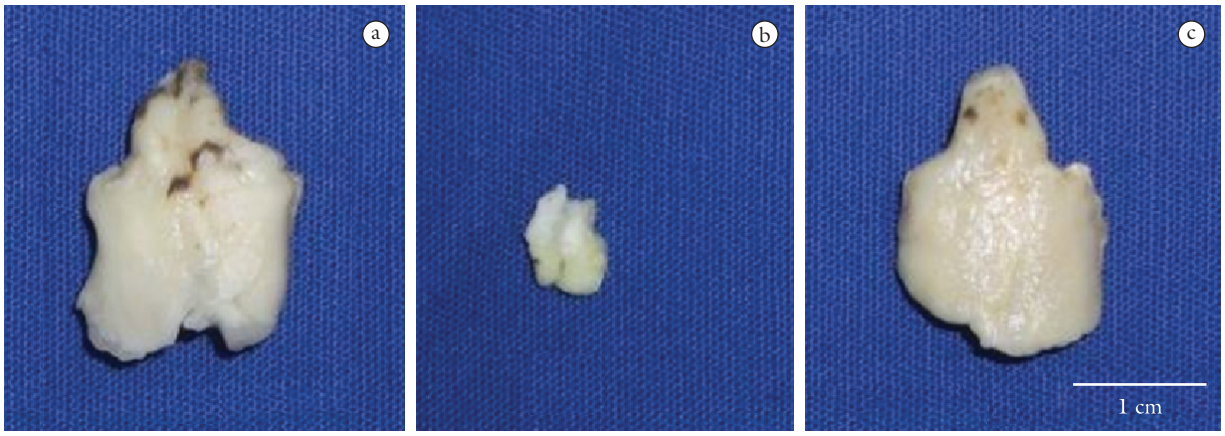

Figure 1. N (a), **UN** (b) and **RN** (c) thymi at 60 days post-natal. **UN** thymi are considerably smaller than **N** and **RN**, undistinguishable among each other. Bilobar configuration is maintained.

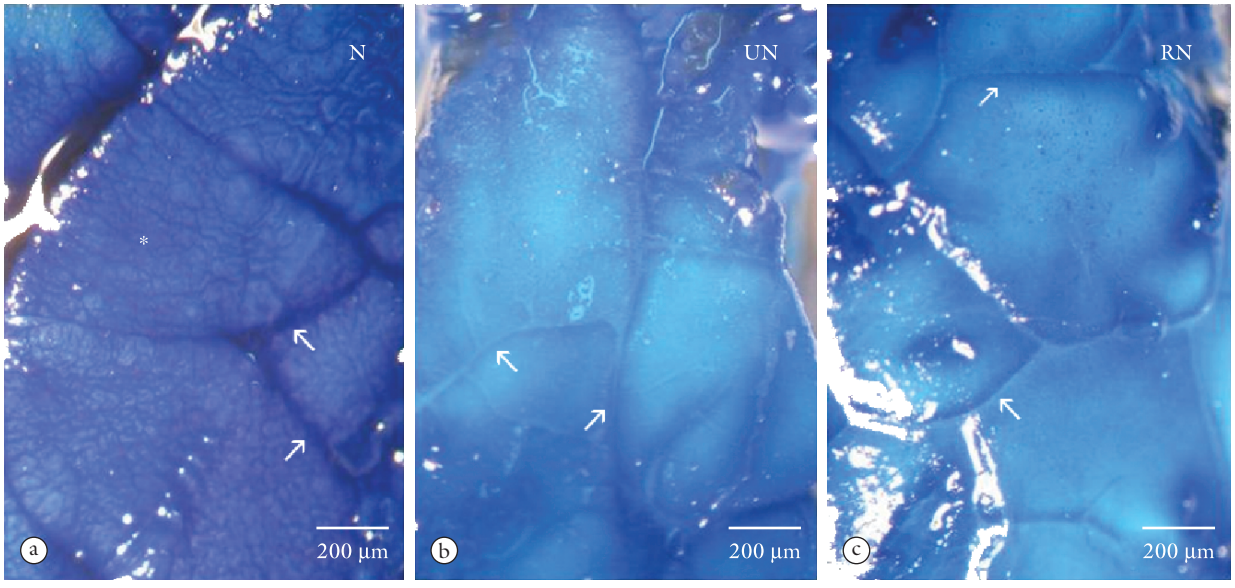

Figure 2. Toluidine Blue-stained **N** (a), **UN** (b) and **RN** (c) thymi. Interlobular septae (arrows) are well-defined in **a** but severely atrophic in **b**. Partial recovery in evident in **c**. Fine surface grooving in **a** (asterisk) represents lymphatic vessels that are absent in **b** and **c**.

3.4 Light microscopy

The significantly different macroscopic appearance of **UN** thymi was further evidenced histologically. The parenchyma of **UN** thymi was clearly distinguishable from those belonging to the **N** group. The corticomedullary boundary was clearly demarcated in both **N** and **RN** thymi; even though some distinction could be made mesoscopically in **UN** thymi, this was clearly lost and there was in fact a wider transition zone between the two layers (Figure 3). Shrunk thymocytes with nuclear debris and fragmentation were found in more external regions that would correspond to the TC of all groups but were clearly more frequent in **UN** animals (Figure 4).

Sirius-red analysis under polarized light revealed most of the thymic capsule in **N** animals was composed of both type I and III collagens – the presence of type III collagen with its green refringence is particularly noticeable (Figure 5a-c). In **N** specimens, type I collagen fibers predominate in the walls of the interlobular vessels with its characteristic red-yellow birefringence (Figure 5c). On the other hand, it is clearly apparent that the red-yellow type I collagen component is increased in the thymic capsule and all septae of **UN** thymi (Figure 5d-f). Further remodeling of the fibrous capsule and septae of the thymus is also evident in the **RN** group – a unique blend of both type I and III collagen results in a remarkable interweaving of green and red-yellow fibers under polarized light (Figure 5g-i) clearly intermediary between the type III pattern of **N** and the type I pattern of **UN** animals. The collagen of interlobular vessels remains unaltered in all groups (Figure 5c, f, i).

3.5 Scanning electron microscopy (SEM)

SEM enabled a thorough spatial analysis of the fibrous component of the thymus. **N** animals had easily identifiable capsules on SEM of a certain thickness as well as sharply demarcated interlobular septae (Figure 6a, b). The

capsules of **UN** thymi, however, were extremely thin and tenuous. Also noted was a paucity of connective tissue in the interlobular septae thus confirming optical microscopy findings (Figure 6c, d). Nearly complete reversal of these alterations is seen in **RN** specimens: a thick capsule and profuse interlobular septae as seen in Figure 6e, f.

3.6 Quantitative analyses

The relative percentages of each component of the thymus (TC, TM and NLT) are exhibited in Table 2. A relative hypotrophy of the TC in **UN** animals was found to be statistically significant but this relation was reverted back to normal in **RN** animals such as vessel density. Compensatory hypertrophy of the TM accompanies TC hypotrophy during the undernutrition phase but had not yet reverted following the renourishment period. These modifications in the lymphoid compartments of the thymus yield a unique distribution for **RN**: while the NLT component is not expected to change in such short time periods of mal- and renourishment, it is expressed in **RN** as a smaller fraction due to TC having recovered while TM still being hypertrophied (Table 2).

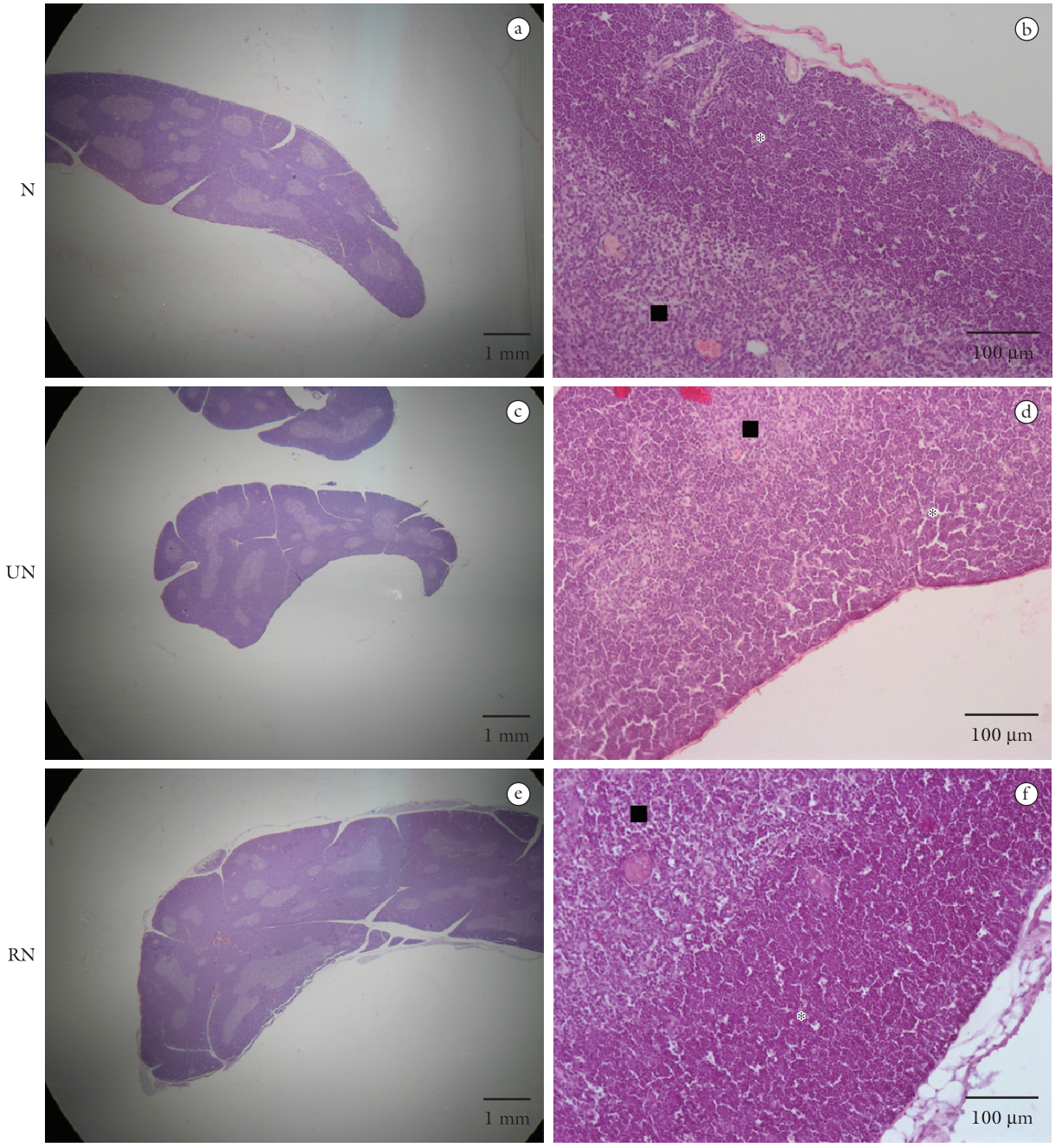

Figure 3. Low- and high-power magnification of HE-stained sections. Low-power photomicrographs (a, c, e) depict the relative size differences and a gross corticomedullary boundary in all three groups. However, examination under high-power magnification (b, d, f) demonstrate that the limit between the cortical (*) and medullary (■) areas is not sharply demarcated in **UN** animals; the usual demarcation is recovered in **RN** specimens.

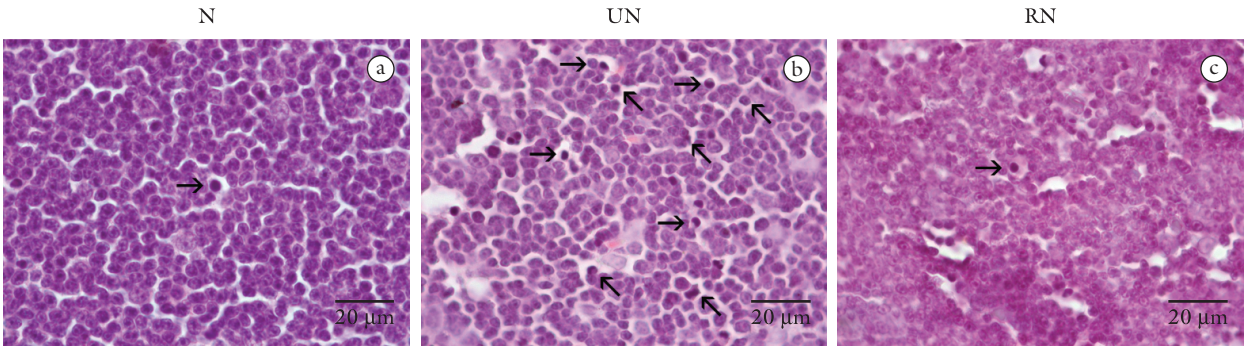

Figure 4. HE-stained sections. Shrunk thymocytes with nuclear fragmentation and debris are highlighted with short arrows. A relative increase in the number of thymocytes with morphological features consistent with apoptosis is evident in UN thymi (b); RN specimens (c), however, cannot be distinguished from N (a).

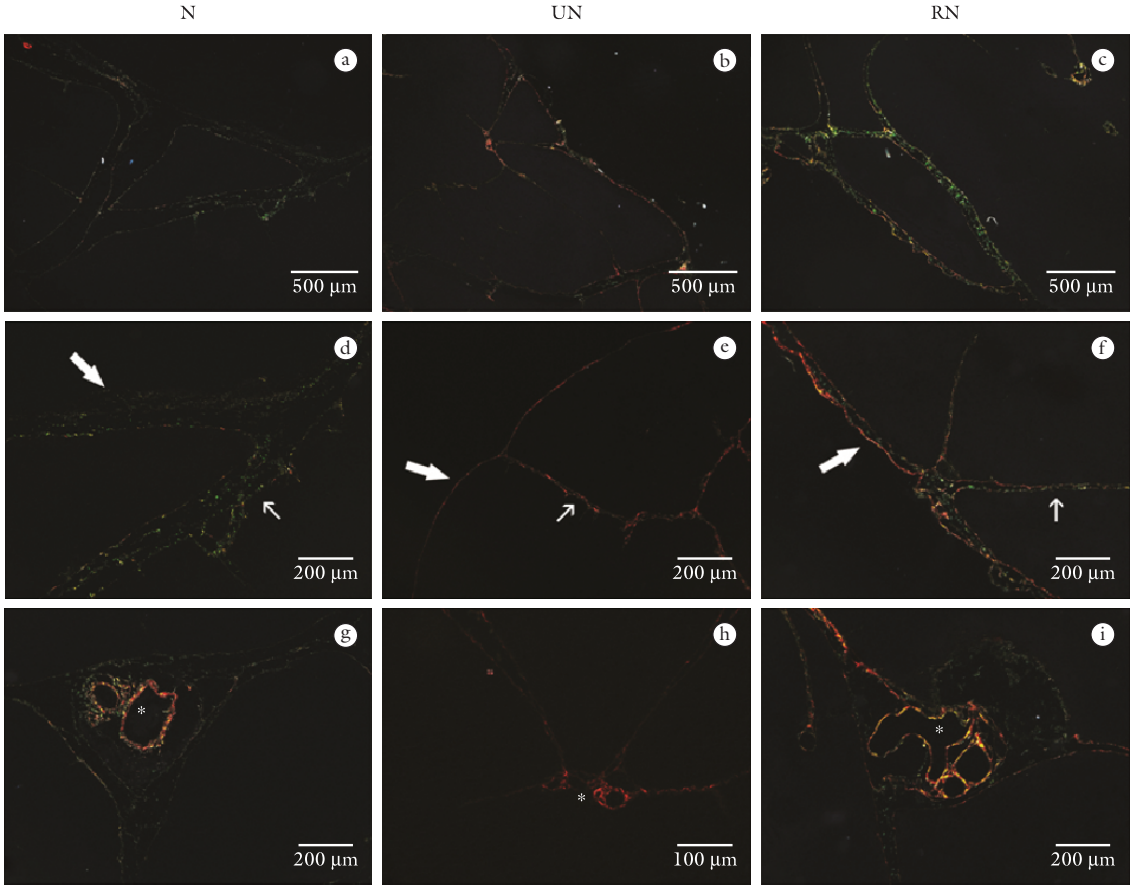

Figure 5. Sirius-Red stained sections, polarized light. a-c) Greenish birefringence indicates a type III collagen predominance in the thymic capsule (thick arrow) and interlobular septae (thin arrow) of **N** specimens. Interlobular vessels demonstrate red-yellow birefringence and thus mostly type I collagen as expected (asterisk). d-f) The thymic capsule (thick arrow) and septae (thin arrow) undergo transformation and red-yellow birefringence is now evident in **UN** animals. This indicates an increase in type I collagen component. g-i) While still demonstrating a remnant of red-yellow birefringence in the thymic capsule (thick arrow), **RN** animals demonstrate more green birefringence (thin arrow) than **UN**, thus indicating restoration of a type III pattern. The collagen of interlobular vessels remains unaltered throughout the three groups (asterisks).

Table 2. Segmental analysis of thymic section areas, mean ± standard deviation. Number in parentheses indicates the stereological coefficient for each vessel density result.

	N	**UN**	**RN**
Cortex (%)	71.8 ± 0.8	68.5 ± 2.1*	71.3 ± 1.2
Medulla (%)	20.2 ± 1.0*	23.3 ± 1.5	23.0 ± 1.0
Non-lymphoid tissue (%)	8.0 ± 0.8	8.3 ± 1.3	5.7 ± 0.6*
Vessel density/mm²	36.3 ± 3.4 (4.18)	11.5 ± 2.0* (7.8)	31.3 ± 6.8 (9.7)

* – $p < 0.05$.

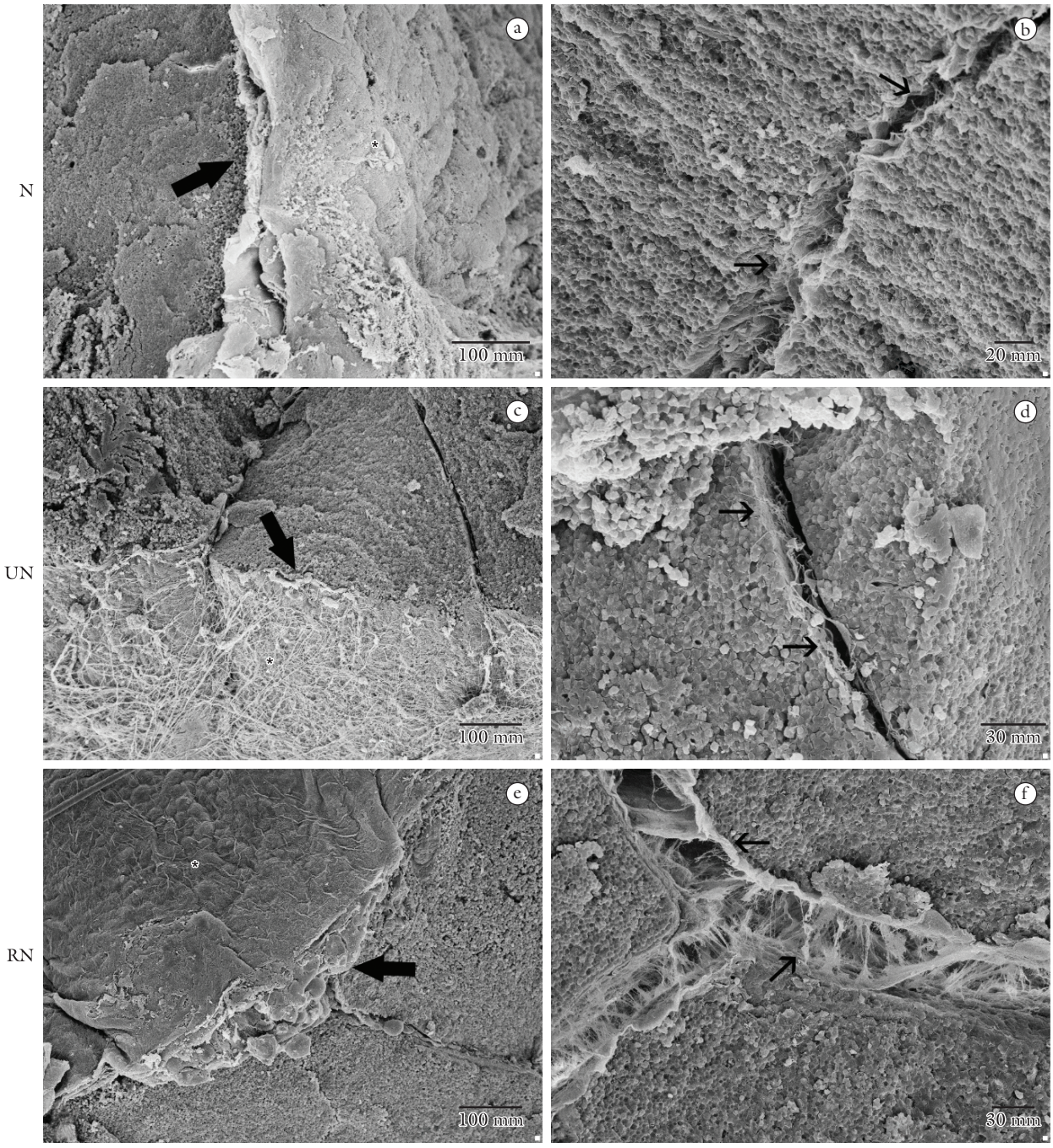

Figure 6. SEM photomicrographs. The thymic capsule external surface is marked by an asterisk. Its relative thickness can be observed (thick arrows) as well as the interlobular septae (thin arrows).

4 Discussion

In this Wistar rat model, perinatal protein undernutrition resulted in an impressive degree of atrophy. Despite the fact that **UN** thymic weight was only 20% of that of the **N** thymi, so was body weight and therefore the thymic/corporal weight ratio remained stable between **N** and **UN**. This decrease in thymic weight had been interpreted before as an isolated phenomenon but is in fact simply part of the global atrophy during protein undernutrition (BARONE, O'BRIEN and STEVENSON, 1993; MITTAL, WOODWARD and CHANDRA, 1988; SAVINO and DARDENNE, 2010). Weindruch and Suffin, on the other hand, reported an increase of the thymic/corporal weight ratio on a caloric-only malnourishment model thus demonstrating the different effects of distinct forms of malnourishment (WEINDRUCH and SUFFIN, 1980) – protein restriction is here shown to have a more profound on thymic morphology. Conversely, protein renourishment led to restoration of thymic weight to values similar to that of the nourished control group even before corporal weight reached baseline values. The differing thymic/corporal weight ratio in **RN** animals indicates a relative thymic hypertrophy following protein renourishment (Table 1).

Diffuse morphological alterations induced by undernutrition are already evident when the thymic capsule is analyzed. These alterations are not mere details in a fibrotic capsule. The clearly-evidenced "grooving" pattern seen in the capsular surface of **N** thymi is composed of fine lymphatic vessels – in fact, their largest concentration is on the surface of this organ and thus an alteration in this component could at least in theory have an important functional implication (KATO, 1997). This pattern was completely lost in **UN** animals and only minimally recovered in **RN** thymi. Further optical microscopy analysis with HE and Sirius-Red stain revealed other qualitative changes involving the **UN** capsule: decreased thickness, absence of septae and almost complete substitution of type III for type I collagen. Once more, morphological changes were only partially reverted with early renutrition – most importantly, collagen composition had already reverted to the **N** pattern thus indicating that 39 days were sufficient for significant connective tissue remodeling inside the thymus. SEM micrographs add evidence to capsular and interlobular septae atrophy during undernutrition and subsequent recovery in the **RN** group.

Even though thymic atrophy is readily evident following protein undernutrition and has been widely reported upon (MITTAL, WOODWARD and CHANDRA, 1988), a per-sector histology analysis reveals some interesting features. The loss of the corticomedullary boundary in **UN** thymi is strikingly similar to the report of Mugerwa (1971) on the thymi of children suffering from Kwashiorkor. Atrophy is not proportional among the 3 different areas of the thymus – **UN** thymi possess a significantly smaller proportion of cortex; the medulla exhibits a consequent relative increase. Correspondingly, increased numbers of shrunk thymocytes with nuclear fragmentation suggesting apoptosis are seen throughout the thymus of **UN** animals but most importantly in more external and peripheric areas where the thymic cortex would have been identified (WATANABE, HITOMI and VAN DER WEE, 2002). Even though not studied here by any method designed to specifically address the proportion of apoptotic cells, it is believed the finding of morphological features classically associated with apoptosis is relevant in the context of pronounced cortical atrophy (ELMORE, 2006; WATANABE, HITOMI and VAN DER WEE, 2002; ZEISS, 2003). Several mechanisms have been identified as playing a role in thymic atrophy during malnutrition with concomitant decrease in the number of mature T lymphocytes – up-regulation of the hypothalamus-hypophysis-adrenal axis and increased levels of circulating corticosteroids are considered to play a major role (BARONE, O'BRIEN and STEVENSON, 1993). Protein renourishment, however, led to a relative increase in the cortical component while the medulla remained stable and NLT drastically decreased. It is evident from this analysis that the cortical component is the most susceptible to protein undernutrition and exhibits the most dramatic response to renourishment. Important functional implications may derive from this fact. The critical steps of thymocytopoiesis take place in the thymus cortex including the settling of lymphocyte stem progenitors and negative lymphocyte selection (GOLDSCHNEIDER, 2006; SAVINO and DARDENNE, 2000; SPRENT and KISHIMOTO, 2002). Relative thymic cortical atrophy may thus be a major morphological correlate to the well-known immundefficient state in protein malnutrition while Savino and Dardenne have already reported that this is mainly due to depletion of the CD4+/CD8+ population subset (SAVINO and DARDENNE, 2010). An important morphofunctional relationship is the correlation between the atrophy on TC of the UN animals and the decrease of vessel density in the TM of these animals. This correlation suggests that functional impairment adversely affecting the migration of mature thymocytes to the bloodstream of **UN** animals exists. This result may provide another morphological substrate to fundament some of the functional immunological impairment seen in subjects suffering from protein-restriction malnutrition. Other functional studies could further analyze these morphological changes; however, subsequent cortical hypertrophy following renourishment suggests that this process is reversible – exactly as observed in the clinical setting (HALE and MARKERT, 2004).

5 Conclusion

The thymus is thus shown to undergo extensive morphological changes following protein malnutrition not limited to the previously described atrophy. Both the lymphoid and non-lymphoid components undergo remodeling that may help explain some of the functional immunological disturbances seen in malnutrition-induced immunodeficiency. Furthermore, the reversal of most of these morphological changes after renutrition is even more impressive and probably the most important result of this study. Particularly encouraging for future research is the relative hypertrophy of the thymus and its cortical layer. In a time when protein malnutrition still affects a significant fraction of the world's population (WATERLOW, 1997), this is a socially- and economically-relevant subject. Additional studies, especially functional assays to assess the presence of an immunological correlate for renourishment-induced morphological recovery, are to be encouraged.

Acknowledgements: We would like to thank Ms. RN Prisco (statistical analysis) and Ms. M Righetti (histology preparations). Partial financial support for this study was obtained from FAPESP – Fundacao de Amparo a Pesquisa do Estado de Sao Paulo. Prof. Liberti is a career investigator of Conselho Nacional de Desenvolvimento Cientifico e Tecnologico (CNPq). Prof. Baptista was the recipient of a graduate student grant from CNPq. The authors do not have any other conflict of interest to disclose. We regret to inform our colleague, Prof. Silvia de Campos Boldrini, has tragically and suddenly passed away in June/2011. Her kindness and hope left permanent marks in our lives.

References

BARONE, KS., O'BRIEN, PC. and STEVENSON, JR. Characterization and mechanisms of thymic atrophy in protein-malnourished mice: role of corticosterone. *Cellular Immunology*, 1993, vol. 148, p. 226-233. PMid:8495490. http://dx.doi.org/10.1006/cimm.1993.1105

BEISEL, WR. History of nutritional immunology: introduction and overview. *Journal of Nutrition*, 1992, vol. 122, p. 591-596. PMid:1542016.

CHANDRA, S. and CHANDRA, RK. Nutrition, immune response, and outcome. *Progress in Food & Nutrition Science*, 1986, vol. 10, p. 1-65. PMid:3097756.

DOUROV, N. Thymic atrophy and immune deficiency in malnutrition. *Current Topics in Pathology*, 1986, vol. 75, p. 127-150. PMid:3514157. http://dx.doi.org/10.1007/978-3-642-82480-7_4

ELMORE, SA. Enhanced histopathology of the thymus. *Toxicology Pathology*, 2006, vol. 34, p. 656-665. PMid:17067951 PMCid:1800589. http://dx.doi.org/10.1080/01926230600865556

GOLDSCHNEIDER, I. Cyclical mobilization and gated importation of thymocyte progenitors in the adult mouse: evidence for a thymus-bone marrow feedback loop. *Immunological Reviews*, 2006, vol. 209, p. 58-75. PMid:16448534. http://dx.doi.org/10.1111/j.0105-2896.2006.00354.x

GREGGIO, FM., FONTES, RB., MAIFRINO, LB., CASTELUCCI, P., DE SOUZA, RR. and LIBERTI, AP. Effects of perinatal protein deprivation and recovery on esophageal myenteric plexus. *World Journal of Gastroenterology*, 2010, vol. 16, p. 563-70. PMid:20128023 PMCid:2816267. http://dx.doi.org/10.3748/wjg.v16.i5.563

HALE, LP. and MARKERT, ML. Corticosteroids regulate epithelial cell differentiation and Hassall body formation in the human thymus. *Journal of Immunology*, 2004, vol. 172, p. 617-624. PMid:14688374.

JUNQUEIRA, LC., TOLEDO, OM. and MONTES, GS. Correlation of specific sulfated glycosaminoglycans with collagen types I, II, and III. *Cell and Tissue Research*, 1981, vol. 217, p. 171-175. PMid:6454491.

KATO, S. Thymic microvascular system. *Microscopic Research and Technique*, 1997, vol. 38, p. 287-299. http://dx.doi.org/10.1002/(SICI)1097-0029(19970801)38:3<287::AID-JEMT9>3.0.CO;2-J

LIBERTI, EA., FONTES, RB., FUGGI, VM., MAIFRINO, LB. and SOUZA, RR. Effects of combined pre- and post-natal protein deprivation on the myenteric plexus of the esophagus of weanling rats: a histochemical, quantitative and ultrastructural study. *World Journal of Gastroenterology*, 2007, vol. 13, p. 3598-604. PMid:17659710.

LIBERTI, EA., VILLA, N., MELHEM, SA., MATSON, E., KÖNIG JUNIOR, B. and ADAMO, J. A morphometrical study of human fetal thymus. *Zeitschrift für mikroskopisch-anatomische Forschung*, 1989, vol. 103, p. 309-315. PMid:2773552.

MANDARIM-DE-LACERDA, CA. *Métodos Quantitativos em Morfologia*. Rio de Janeiro: UERJ, 1995. 131 p.

MELROSE, J., SMITH, SM., APPLEYARD, RC. and LITTLE, CB. Aggrecan, versican and type VI collagen are components of annular translamellar crossbridges in the intervertebral disc. *European Spine Journal*, 2007, vol. 17, p. 314-324. PMid:17972112 PMCid:2365556. http://dx.doi.org/10.1007/s00586-007-0538-0

MITTAL, A. and WOODWARD, B. Thymic epithelial cells of severely undernourished mice: accumulation of cholesteryl esters and absence of cytoplasmic vacuoles. *Proceedings of the Society for Experimental Biology and Medicine*, 1985, vol. 178, p. 385-391. PMid:2579402.

MITTAL, A., WOODWARD, B. and CHANDRA, RK. Involution of thymic epithelium and low serum thymulin bioactivity in weanling mice subjected to severe food intake restriction or severe protein deficiency. *Experimental and Molecular Pathology*, 1988, vol. 48, p. 226-235. http://dx.doi.org/10.1016/0014-4800(88)90059-7

MIYAI, K., ABRAHAM, JL., LINTHICUM, DS. and WAGNER, RM. Scanning electron microscopy of hepatic ultrastructure: secondary, backscattered, and transmitted electron imaging. *Laboratory Investigation*, 1976, vol. 35, p. 369-376. PMid:979166.

MONTES, GS., KRISZTÁN, RM. and JUNQUEIRA, LC. Preservation of elastic system fibers and of collagen molecular arrangement and stainability in an Egyptian mummy. *Histochemistry*, 1985, vol. 83, p. 117-119. PMid:2412989. http://dx.doi.org/10.1007/BF00495140

MUGERWA, JW. The lymphoreticular system in Kwashiorkor. *Journal of Pathology*, 1971, vol. 105, p. 105-109. PMid:4109254. http://dx.doi.org/10.1002/path.1711050204

PELLETIER, DL. The potentiating effects of malnutrition on child mortality: epidemiologic evidence and policy implications. *Nutrition Reviews*, 1994, vol. 52, p. 409-415. PMid:7898782.

REEVES, PG., NIELSEN, FH. and FAHEY, GC. Purified diets for laboratory rodents: final report of the American Institute of Nutrition Ad Hoc Writing Committee on the reformulation of the AIN-76A rodent diet. *Journal of Nutrition*, 1993, vol. 123, p. 1939-1951. PMid:8229312.

REVILLARD, JP. and COZON, G. Experimental models and mechanisms of immune deficiencies of nutritional origin. *Food Additives and Contaminants*, 1990, vol. 1, p. S82-86. 7 Supplement.

ROMEIS, B. *Mikroskopiche Technik*. Munchen: Baltimore, 1968. 697 p.

SAVINO, W. and DARDENNE, M. Nutritional imbalances and infections affect the thymus: consequences on T-cell-mediated immune responses. *The Proceedings of the Nutrition Society*, 2010, vol. 69, p. 636-643. PMid:20860857. http://dx.doi.org/10.1017/S0029665110002545

SAVINO, W. and DARDENNE, M. Neuroendocrine control of thymus physiology. *Endocrinology Reviews*, 2000, vol. 21, p. 412-443. http://dx.doi.org/10.1210/er.21.4.412

SCHNEEBERGER-KEELEY, EE. and KARNOVSKY, MJ. The ultrastructural basis of alveolar-capillary membrane permeability to peroxidase used as a tracer. *The Journal of Cell Biology*, 1968, vol. 37, p. 781-793. PMid:11905208 PMCid:2107447. http://dx.doi.org/10.1083/jcb.37.3.781

SCHOFIELD, C. and ASHWORTH, A. Why have mortality rates for severe malnutrition remained so high? *Bulletin World Health Organization*, 1996, vol. 74, p. 223-229. PMid:8706239 PMCid:2486901.

SIMON, J. *A physiological essay on the thymus gland*. London: Renshaw, 1845.

SLOBODIANIK, NH., PALLARO, AN., ROUX, ME. and RIO, ME. Effect of low-quality dietary protein on the thymus of growing rats. *Nutrition*. 1989, vol. 5, p. 417-418. PMid:2520336.

SPRENT, J. and KISHIMOTO, H. The thymus and negative selection. *Immunological Reviews*, 2002, vol. 185, p. 126-135. PMid:12190927. http://dx.doi.org/10.1034/j.1600-065X.2002.18512.x

SWEAT, F., PUCHTLER, H. and WOO, P. A light-fast modification of Lillie's allochrome stain. Periodic acid-schiff-picro-sirius blue gl. *Archives of Pathology*, 1964, vol. 78, p. 73-75. PMid:14148751.

WALKER, A., NAKAMURA, T. and HODGSON, D. Neonatal lipopolysaccharide exposure alters central cytokine responses to stress in adulthood in Wistar rats. *Stress*, 2010, vol. 13, p. 506-515. PMid:20666652.

WATANABE, M., HITOMI, M. and VAN DER WEE, K. The pros and cons of apoptosis assays for use in the study of cells, tissues, and organs. *Microscopy and Microanalysis*, 2002, vol. 8, p. 375-391. PMid:12533214. http://dx.doi.org/10.1017/S1431927602010346

WATERLOW, JC. Protein-energy malnutrition: the nature and extent of the problem. *Clinical Nutrition*, 1997, vol. 1, p. 3-9. 16 Supplement.

WEIBEL, ER. *Stereological methods*: Practical methods for biological morphometry. New York: Academic Press, 1979. 415 p.

WEINDRUCH, RH. and SUFFIN, SC. Quantitative histologic effects on mouse thymus of controlled dietary restriction. *Journal of Gerontology*, 1980, vol. 35, p. 525-531. PMid:7400544. http://dx.doi.org/10.1093/geronj/35.4.525

ZAR, J. *Biostatistical analysis*. Upper Saddle River: Prentice Hall, 1999. 929 p.

ZEISS, CJ. The Apoptosis-Necrosis Continuum: Insights from Genetically Altered Mice. *Veterinary Pathology*, 2003, vol. 40, p. 481-495. PMid:12949404. http://dx.doi.org/10.1354/vp.40-5-481

Received September 12, 2012
Accepted February 15, 2013